Fungi present distinguishable isotopic signals in their lipids when grown on glycolytic versus tricarboxylic acid cycle intermediates

Stanislav Jabinski[1,2] Vítězslav Kučera[3,4], Marek Kopáček[1,5], Jan Jansa[4], Travis B. Meador[1,2,5*]

[1]University of South Bohemia, Faculty of Science, Department of Ecosystem Biology, Branišovská 1760, 370 05 České Budějovice, Czechia

[2]Institute of Soil Biology and Biochemistry, Biology Centre CAS, Na Sádkách 7, 370 05 České Budějovice, Czechia

[3]Charles University, Faculty of Sciences, Albertov 6, 128 00 Praha, Czechia

[4]Institute of Microbiology CAS, Vídeňská 1083, 142 20 Praha, Czechia

[5]Institute of Hydrobiology, Biology Centre CAS, Na Sádkách 7, 370 05 České Budějovice, Czechia

Correspondence to: Travis B. Meador (travis.meador@bc.cas.cz)

Abstract. Microbial activity in soils controls both the size and turnover rates of large carbon (C) inventories stored in the subsurface, having important consequences for partitioning of C between terrestrial and atmospheric reservoirs as well as recycling of mineral nutrients such as nitrogen or phosphorus (often bound to the C) that support plant growth. Fungi are major decomposers of soil organic matter (SOM); however, uncertainty about the identity of predominant C substrates that fuel their respiration confound models of fungal production and SOM turnover. To further define the signals of microbial heterotrophic activity, we applied a dual hydrogen (H) and C stable isotope probing (SIP) approach on pure fungal cultures representing the phyla Ascomycota, Basidiomycota, and Zygomycota growing on monomeric (glucose, succinate) or complex substrates (tannic acid, β-cyclodextrin). Our findings demonstrate that the investigated species incorporated only minor amounts of inorganic C (provided as bicarbonate) into their membrane lipids, amounting to < 3% of lipid-C, with no consistent patterns observed between species or growth substrates. The net incorporation of water-derived H (i.e., ~~a_w~~a_w) into lipids also did not differ significantly between incubations with monomeric versus complex substrates; however, growth on succinate ~~solicited~~ elicited significantly higher ~~a_w~~a_w values than glucose or β-cyclodextrin. This finding suggests that ^{2}H-SIP assays have the potential to distinguish between microbial communities supported predominantly by substrates that are catabolized by the tricarboxylic acid cycle versus glycolytic pathway. Furthermore, the average ~~a_w~~a_w value of heterotrophic fungal incubations [0.69 ± 0.03 (SEM)] is consistent with that observed for bacterial heterotrophs, and may be applied for upscaling lipid-based estimates of fungal production in environmental assays.

Short Summary

Microbial production is a key parameter in estimations of organic matter cycling in environmental systems, and fungi play a major role as decomposers. In order to investigate fungal production and turnover times in soils, we incubated fungal pure cultures with isotopically labelled water and bicarbonate to investigate growth signals encoded into lipid biomarkers, which can be applied to improve flux estimates in environmental studies.

1 Introduction

Soil organic matter (SOM) is the major reservoir of carbon (1580×10^{15} g C) in the biosphere, and active microbial populations act to redistribute this C to other reactive reservoirs, such as the atmosphere (Carson et al., 2001; Grinhut et al., 2007). Major uncertainties in modeling C and climate dynamics stem from insufficient knowledge on the controls of SOM degradation and transformation (Ciais et al., 2014; Lindahl and Tunlid 2015). Saprotrophic soil fungi are one of the major decomposers in soils, are known to degrade naturally occurring complex molecules such as lignin (Kirk & Farrell, 1987; Fioretto et al., 2005; Baldrian et al., 2011), cellulose (Šnajdr et al., 2011) and humic substances (Grinhut et al., 2007), but are also reported to compete for accessible plant photosynthate excreted by roots (De Boer et al., 2005; Högberg et al., 2001; Smith & Read, 2008). Despite the unique and important fungal niche in biogeochemical cycles, their contributions to SOM cycling remains poorly constrained (Frey 2019; Grinhut et al., 2007). Furthermore, heterotrophic organisms feeding on organic substrates to gain energy and build biomass are also known to fix a variable amount of inorganic C (IC), in order to replenish intermediates in the tricarboxylic acid (TCA) cycle (Kornberg 1965). It has been suggested that 2 - 8% of the biomass C in heterotrophs originates from IC incorporated through anaplerotic carboxylation reactions (Romanenko 1964; Roslev et al., 2004; Braun et al., 2021). Awareness of these processes has existed for decades (Kornberg 1965; Sorotkin 1966). Yet, the relevance and metabolic controls on heterotrophic IC fixation remains poorly understood, partly due to the lack of reliable estimates for most organisms and habitats (Braun et al., 2021).

Advanced analytical techniques now allow microbial taxa to be linked to specific processes in environmental studies by measuring incorporation of stable isotopes into biomarkers (Boschker et al., 1998; Dumont and Murrell, 2005; Kreuzer-Martin, 2007), such as fungal and bacterial membrane lipid fatty acids (Treonis et al., 2004; Willers et al., 2015) or other biomarkers (Boschker and Middelbourg, 2002). Previous studies have demonstrated that variability in the $^{2/1}$H composition of microbial lipids is redundant with that of environmental water (Hoefs, 2018; Kopf et al., ~~2015~~2016), and stable isotope probing (SIP) assays applying enrichments in ^{2}H$_2$O have proven to be a useful tracer of microbial activity in a diverse range of environments (Canarini et al., 2024; Caro et al., 2023; Fischer et al., 2013; Kellermann et al., 2012; Wegener et al., 2016; Warren 2022; Wu et al., 2018). It is important to distinguish these ^{2}H-labeling applications from parallel investigations aiming to determine the ~~Large~~ kinetic and equilibrium isotope ~~H-isotope~~ fractionations ~~, yielding δ^2H values between −400‰ and +200‰,~~resulting ~~from~~ ~~have been observed during~~ biosynthetic incorporation of water hydrogen (water-H) into individual compounds ~~within a single cell or total biomass~~(i.e., ε; cf. Hayes 2004). While ε~~, which~~ values can be indicative of ~~the~~ an underlying metabolic

2

64   processes or environmental change (Osborn et al., 2011; Sachse et al., 2012; Zhang et al., 2009), the large range of ε that have

65   been reported for fatty acids of aerobic, heterotrophic bacteria [-330 > ε > +360 ‰; see review by Pilecky et al. (2025)] arise,

66   in part, because water-H is not the only source of H for biomolecules, complicating the interpretation of such values observed

67   in natural systems. In contrast, the water-H incorporation factor (or water-H assimilation efficiency; a_w) accounts for variability

68   in the proportion of H derived from water as well as $^{2/1}H$ fractionation during biosynthesis (cf. Zhang et al., 2009; Kopf at al.

69   2015; see Methods), and has been valuable for SIP approaches to (*i*) estimate microbial production rates in natural systems

70   (e.g., Wegener et al., 2022; Caro et al., 2023), and (*ii*) establish characteristic growth patterns of microbial populations that can

71   access a large diversity of substrates, such as methanogens (Wu et al., 2020).

72   To fully exploit the potential of SIP experiments, a dual-SIP approach was developed to track total microbial production by

73   adding heavy water (^2H_2O) together with ^{13}C-labeled IC, enabling simultaneous estimates of total and autotrophic metabolism,

74   respectively (Wegener et al., 2012; Wu et al., 2020). Recently, Jabinski et al. (2024) validated an innovation of the dual-SIP

75   assay by using rapid pyrolysis of fungal biomass to determine the stable C and H isotopic composition of fungal lipids, and

76   demonstrated that water-H and IC assimilation signatures could successfully distinguish between fungal ecotypes growing on

77   glucose or glutamic acid as the C source. The aim of the current study was to further assess the controls on water-H and IC

78   incorporation into lipids and expand our knowledge for interpreting environmental signals by applying the dual-SIP assay on

79   a broader range of pure fungal cultures and growth substrates, including labile monomers versus more complex, high molecular

80   weight molecules. We hypothesized that (*i*) the incorporation of IC and water-H into the fungal fatty acid biomarker $C_{18:2}$ will

81   be similar for fungal species growing on the same substrate, and (*ii*) that IC and water-H incorporation will distinguish between

82   growth on labile versus more complex C substrates.

83   **2 Methods**

84   **2.1 Cultivation & Harvesting**

85   Fungal pure cultures of two Basidiomycota [*Paxillus involutus* (PI, strain SB-22); *Phanerodontia chrysosporium* (PC, strain

86   CCM8074)], two Zygomycota [*Mortierella* sp. (MO, strain RK-38); *Umbelopsis* sp. (UM, strain RK-43)] and two Ascomycota

87   [*Penicillium janczewskii* (PJ, strain BCCO20_0265); *Paecilomyces lilacinus* (PL, strain DP-23)] were incubated in 500 mL

88   Schott bottles at 25 °C in the dark. Liquid mineral media (50 mL) was adapted after Bukovská et al. (2018) with the vitamins

89   left out, and was inoculated with approximately 10^6 spores, or, for Basidiomycota, a hyphal block < 0.5 cm^3 recovered from a

90   previous culture using the same cultivation medium solidified with agar (1.5%).

91   The growth medium contained per liter: 4 g organic C in various forms ($C_6H_{12}O_6$ glucose; $C_4H_6O_4$ succinic acid; $C_{42}H_{70}O_{35}$ β-

92   Cyclodextrin or $C_{76}H_{52}O_{46}$ tannic acid), 0.01 g $FeSO_4$ * $7H_2O$, 2 g KH_2PO_4, 0.5 g $MgSO_4$ * $7H_2O$, 0.1 g NaCl, 0.1 g CaCl, 2.5

93   g $(NH_4)_2SO_4$, 0.45 g $NaHCO_3$ and 1 mL of a mixed solution (per liter: 0.5 g H_3BO_3, 0.04 g $CuSO_4$ * $5H_2O$, 0.1 g KI, 0.4 g

94    $MnSO_4$ * $5H_2O$, 0.2 g $NaMoO_4$ * $2H_2O$, 0.4 g $ZnSO_4$ * $7H_2O$). The pH of the medium was adjusted to 4.5 before inoculation.

95   Dual-SIP experiments were performed using ^{13}C-bicarbonate (^{13}C-DIC, $NaH^{13}CO_3$) and deuterated water (^2H_2O). Each

96 fungal strain was grown in triplicate with non-labeled substrates (Treatment I), with δ^2H of the medium water adjusted to 100‰

97 and AT^{13}C = 10% of ^{13}C-DIC (Treatment II), 200‰ δ^2H and 10% ^{13}C-DIC (Treatment III), and 400‰ δ^2H and 10% ^{13}C-DIC

98 (Treatment IV). The concentration of the bicarbonate in the cultivation medium was 0.1 g L^{-1}. The Schott bottles were closed

99 with a rubber stopper in order to prevent the labeled ^{13}C-DIC from outgassing, and ample headspace was provided to maintain

100 oxic conditions throughout the growth experiment. Fungal growth was monitored via the accumulation of CO_2 in the

101 headspace, and we aimed to harvest when CO_2 levels reached 10%; however, without preliminary knowledge of the fungal

102 growth dynamics, some cultivations exceeded this level more quickly than they could be harvested.

103 To harvest the fungal biomass, mycelia were separated from the growth medium via vacuum filtration through 5 μm Isopore

104 polycarbonate filters (47 mm diam, Merck catalogue number TMTP04700) and the cultivation medium was collected into a

105 sterile 50 mL tube. Thereafter, the mycelium was washed with ample MilliQ water, transferred to pre-weighed, sterile 50 mL

106 tubes; the fresh weight of the biomass was recorded, and the samples were frozen at -80 °C until lyophilization. A subsample

107 of the cultivation medium was also frozen at -80 °C and the rest was used to determine pH post-incubation. After lyophilization,

108 the dry weight of each sample was determined and stored at -20 °C until further analysis.

109

110 **2.2 Measurements**

111 **2.2.1 Headspace CO_2 concentration and isotope composition**

112 Samples of headspace (0.3 mL) were collected weekly from each bottle into helium flushed 12 mL exetainer vials (Exetainer,

113 Labco Limited, UK) and analyzed for their CO_2 concentration and $^{13}C/^{12}C$ isotopic ratio using GasBench II equipped with a

114 single cryo-trap connected to Delta V Advantage isotopic ratio mass spectrometer (IRMS) via Conflo IV (Thermo Scientific,

115 Bremen, Germany). Ambient air (with its CO_2 concentration measured using LiCor 850 gas analyzer previously) was used as

116 a standard for CO_2 concentration measurements, whereas a laboratory cylinder with 0.1% CO_2 in helium was used as a standard

117 for isotopic composition ($\delta^{13}C$ = -2.86 ‰). The analytical precision was below 1‰. Data were analyzed and exported using

118 Isodat 3.0 software.

119 **2.2.2 Medium water (^2H_2O)**

120 Liquid samples were transferred into 1.5 ml glass vials (32 x 11.6 mm, Fischer Scientific) and then measured using Triple

121 Liquid Water Isotope Analyzer (Los Gatos Research), which is based on the principle of high-resolution laser absorption

122 spectroscopy. Samples were dispensed into the instrument using an autosampler (PAL3 LSI, ABB company) and a 1.2 μL

123 syringe (Hamilton). Samples were measured and evaluated against prepared laboratory standards of known isotopic

124 composition. The isotopic ratios of these laboratory standards were verified by measuring against international standards

125 (VSMOW2, SLAP2) made by the IAEA. For quality control purposes, the measurements of the samples were also interspersed

with periodic measurements of the prepared verification samples with known isotopic composition. The final isotopic composition (δ^2H) was determined using LIMS software. Analytical precision of δ^2H was <1.5‰.

Water sampled from incubations with tannic acid could not be measured using the laser, as described above, due to its high organic carbon content, and was rather measured via a GasBench II device (Thermo Scientific, Bremen, Germany; Application Note: 30049). Medium water samples (200 µL) were added with a platinum catalyst to a 12 mL exetainer vials (Exetainer, Labco Limited, UK). The headspace was flushed with 1% H_2 in He at approximately 100 mL min^{-1} for 6 min. After an equilibration time of over 40 min, the samples were measured by purging the exetainer using a double-holed needle with helium into a 250 µL sample loop. The sample was then injected and separated via a Carboxen PLOT 1010 (0.53 mm ID; Supelco, Bellefonte, USA) held at 90 °C with a flow rate of ~2.2 mL min^{-1}, and then introduced into the MAT253 Plus IRMS via a Conflo IV interface. Each sample was injected three times during one analysis. The isotopic composition was determined using Isodat 3.0 software against the corresponding H_2 working gas (-239‰ for δ^2H) and the values were corrected and normalized using international standards VSMOW2 (0‰ for δ^2H), SLAP2 (-427.5‰ for δ^2H), USGS53 (+40.2‰ for δ^2H) and GFLES-2 (159.9‰ for δ^2H). The analytical precision was around 1‰.

2.2.3 Carbon (δ^{13}C) substrate analysis

Substrates (~100 µg) were weighed into tin capsules (8 × 5 mm, Sercon, Crewe, UK) and placed in a helium-flushed carousel autosampler, then introduced to an Elemental Analyzer IsoLink device (EA IsoLink CNSOH, Thermo Scientific, Bremen, Germany) equipped with a CHN/NC/N EA combustion/reduction reactor (Sercon, Crewe, UK) heated to 1020 °C. A pulse of oxygen was introduced to the reactor simultaneously with the sample. The sample gases were quantified via a thermal conductivity detector (TCD) and then introduced to a MAT 253 Plus isotope ratio mass spectrometer (IRMS; Thermo Scientific; Bremen, Germany) via the open split of a Conflo IV interface, with helium as the carrier gas. The isotopic composition was determined using Isodat 3.0 software against the corresponding CO_2 working gas (-4.191‰ for δ^{13}C), and the values were corrected for linearity and normalized to the VPDB scale using international reference material IAEA-600 (-27.771‰ for δ^{13}C). The analytical precision was <0.04‰.

2.2.3 Pyrolysis GC for lipid analysis

The pyrolysis unit Shimadzu 3030D (Shimadzu, Kyoto, Japan/ Frontier Laboratories, Fukushima, Japan) was installed on top of the GC Trace1310 gas chromatograph SSL injector (Thermo Scientific, Bremen, Germany) and the GC was equipped with an SLB-IL60 column (non-bonded; 1,12-Di(tripropylphosphonium)dodecane bis(trifluoromethanesulfonyl)imide phase, 30 m, 0.25 mm ID, 0.20 µm df, Supelco, Bellefonte, USA). The furnace temperature was 650 °C and the interface temperature was 370 °C. The injector temperature was 360 °C and the GC oven was held at 80 °C for 1 min then ramped to 175 °C at 15 °C min^{-1}, then ramped to 195 °C at 2 °C min^{-1}, then ramped to 300 °C at 10 °C min^{-1}, and finally held at 300 °C for 7 min. Helium

was used as the carrier gas, with a constant flow of 1.5 mL min^{-1}, a split ratio of 40, and a split flow of 26.7 mL min^{-1}. The column flow was split via a multichannel device to acquire MS and isotopic data simultaneously from one injection. The GCMS (ISQ QD; Thermo Scientific, Bremen, Germany) ion source was set to electron impact ionization mode (EI) at 70 eV and a scan range of m/z 50 – 500 with a scan time of 0.2 sec^{-1}. Scanning started after 8 min to avoid the solvent peak in the MS. The transfer line temperature was set to 300 °C and the ion source was set to 250 °C.

The samples (lyophilized biomass, 0.1 – 1.3 mg) were weighed into an ultra-clean stainless steel Eco-Cup LF (Frontier Laboratories, Fukushima, Japan), which were burned with a torch before usage to remove contaminants. Immediately prior to sample injection, 30 μL of trimethylsulfonium hydroxide (TMSH) was added on the sample to increase the volatization by transforming the fatty acids into fatty acid methyl esters (FAMEs) ~~of the fatty acids~~ and improve measurement sensitivity. Identification of ~~fatty acid methyl esters (~~FAMEs~~)~~ was performed using fragmentation patterns and the NIST 14 library. Stable ~~carbon~~ C and ~~hydrogen~~ H isotope compositions of FAMEs from ~~the~~aliquots of the same biomass ~~were~~ separately determined by splitting the flow from the GC column to a GC-IsoLink II reactor, coupled to a MAT253 Plus IRMS via a Conflo IV interface. Values are expressed in standard delta notation (δ^{13}C and δ^{2}H). MS information was simultaneously acquired by use of the multi-channel device described above. For conversion of FAMEs and ergosterol to CO_2, the combustion reactor (nickel oxide tube with CuO, NiO, and Pt wires) was set to 1000 °C. For conversion of FAMEs and ergosterol to H_2, the pyrolysis reactor (aluminum tube) was set to 1420 °C. The FAMEs were identified by their retention times and fragmentation patterns. The isotopic composition was determined using Isodat 3.0 software against the corresponding CO_2 or H_2 working gas (-4.191‰ for δ^{13}C, -239.5‰ for δ^{2}H). Isotope corrections for instrument drifts, linearity, and normalization to the VPDB or VSMOW scales were performed according to the response of USGS70 (-30.53‰ for δ^{13}C, -183.9‰ for δ^{2}H) and USGS72 (-1.54‰ for δ^{13}C, 348.3‰ for δ^{2}H) reference standards. The analytical precision was < 0.5‰ and < 10‰ for δ^{13}C and δ^{2}H, respectively.

2.3 Calculations

Carbon use efficiency (CUE) for the growth experiments was calculated by normalizing the amount of C in biomass by that plus C that accumulated as CO_2 [CUE = biomass-C / (CO_2-C + biomass-C)]. The δ^{13}C values of fungal biomarker $C_{18:2}$ was ~~determined as~~determined as standard delta values (‰). The IC incorporation into the biomarker (%IC) was calculated based on the following equation:

$$\%IC_{(assimilation)} = \frac{{}^{13}F_{lipid} - {}^{13}F_{lipid,control}}{{}^{13}F_{DIC(medium)} - {}^{13}F_{substrate}} \times 100 \qquad \textbf{(Eq. 1)}$$

Equation 1: Inorganic carbon (%IC) assimilation was calculated as the difference in the ^{13}C atom fraction of the lipids harvested at the end of the labeling experiment (^{13}F$_{lipid}$) compared to the lipids harvested at the end of the natural abundance treatment (^{13}F$_{lipid,control}$), relative to the difference between the mixing-weighted average ^{13}C atom fraction of dissolved inorganic C (^{13}F$_{DIC}$, cf. Text S1) and the ^{13}F of the substrate. F was calculated as ^{13}F = (R$^{13/12}$)/(R$^{13/12}$ + 1), where R is re-calculated from the δ^{13}C ratios

189 **reported by Isodat Software following measurement by IRMS ($\delta^{13}C$ = ([$R^{13/12}$]$_{sample}$/[$R^{13/12}$]$_{ref}$ - 1) * 1000 (modified after Boschker**

190 **& Middelburg 2002; Wegener et al., 2012).**

191 The water H assimilation efficiency (~~a_w~~a_w) for fungal biomarker $C_{18:2}$ was approximated from the regressions of the hydrogen

192 isotope composition of individual fatty acids $^2F_{FA}$ and that of medium water ($^2F_{water}$), according to Kopf et al. (~~2015~~2016), after

193 Zhang et al. (2009). Briefly, the hydrogen isotopic compositions of microbial fatty acids produced by an organism generally

194 follow the isotopic composition of environmental water, and are related to the mole fraction of H contributed from water in

195 the cultivation medium (~~x_w~~f_W) and the net hydrogen isotope fractionation between fatty acids and water ($\alpha_{fa/w}$), where ~~a_w~~a_w =

196 ~~x_w~~f_w × $\alpha_{fa/w}$. Whereas a_W can be determined experimentally, the latter terms cannot be independently determined for

197 heterotrophic growth (Kopf et al., ~~2015~~2016). The traditional isotope effects and $\varepsilon_{C18:2/water}$ and $\alpha_{C18:2/water}$ were calculated after

198 Hayes (2004), where $\alpha_{C18:2/water}$ = [($\delta^2H_{C18:2}$ + 1000) / (δ^2H_{water} +1000)] and $\varepsilon_{C18:2/water}$ = ($\alpha_{C18:2/water}$ -1) × 1000‰.

199 Notably, calculation of %IC and a_w consider relative increases in $^{13/12}C$ or $^{2/1}H$ composition, and thus do not require a correction

200 for the methyl group added during derivatization of the fatty acid. The $\varepsilon_{C18:2/water}$ values determined in this study were not

201 corrected for the additional methyl group and add an inaccuracy to the reported values, as further discussed below.

202

203 **3 Results**

204

205 **3.1 Fungal growth and CO_2 production**

206 All fungal species were pure cultures, which were incubated in a mineral medium with either glucose, succinate, β-cyclodextrin,

207 or tannic acid serving as the sole organic C source. Growth was monitored by the evolution of CO_2 into the headspace, which

208 ranged from 0.36% (no respiration of substrate) to a maximum of 35%, after incubation times ranging from 5 to 160 days (Fig.

209 1). The pH of the media in all incubations ranged from 2 to 5.5 at the time of harvest, with a general trend of decreasing pH

210 with increasing CO_2; however, the trend was opposite when succinate was the carbon source, with pH increasing from 4 to

211 5.5. For samples that produced sufficient biomass, the dry biomass of harvested fungal hyphae ranged up to 250 mg, and at

212 least 30 µg dry biomass was used to analyze fungal membrane fatty acids by Pyr-GC-IRMS. Only the Ascomycota species PL

213 and PJ grew sufficiently on each tested substrate to produce enough biomass for stable isotope analysis. Incubations of

214 Zygomycota species with glucose or succinate also yielded sufficient dry biomass, and only UM was able to grow on β-

215 cyclodextrin. Zygomycota species produced neither CO_2 nor biomass when incubated with tannic acid. The Basidiomycota

216 typically exhibited the slowest growth, and both species (PI and PC) only produced enough biomass when grown on glucose.

217 The headspace CO_2 levels in Basidiomycota incubations with succinate increased to a maximum of ~ 2%, but only PI yielded

218 sufficient biomass for analysis. PC grew sufficiently on β-cyclodextrin, with CO_2 levels increasing to a maximum of 3%, while

219 CO_2 remained < 0.6% in PI incubations.

220

Glucose

Succinate

Tannic acid

Beta-Cyclodextrin

(PL)   (PI)   (UM)
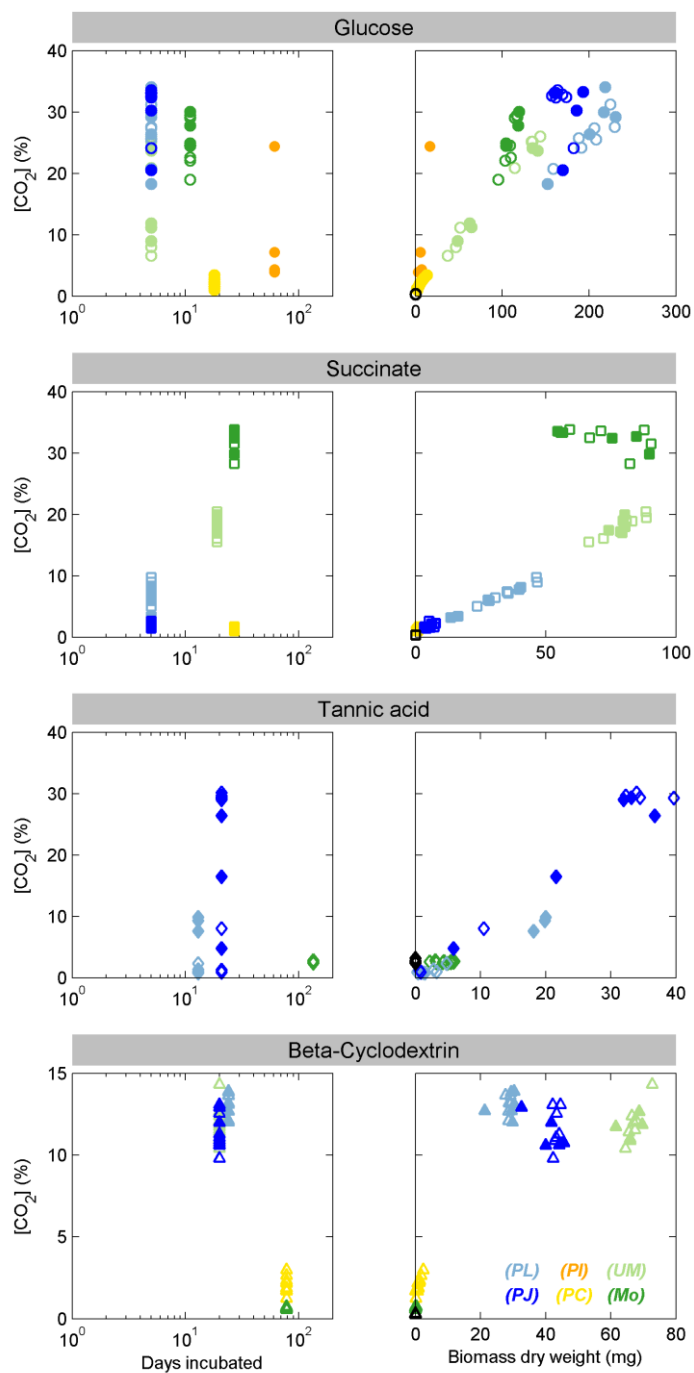(PJ)   (PC)   (Mo)

Days incubated

Biomass dry weight (mg)

221

222 **Figure 1. Growth of fungal species on each substrate as indicated by production of CO_2 versus days of incubation (left panels) or dry**
223 **biomass (right panels). Filled symbols indicate samples for which the $C_{18:2}$ biomarker was measured by Pyr-GC-IRMS. Colors**
224 **represent the Ascomycota species *Penicillium janczewskii* (PJ, dark blue) and *Paecilomyces lilacinus* (PL, light blue), Zygomycota**
225 ***Mortierella* sp. (MO, dark green) and *Umbelopsis* sp (UM, light green), and Basidiomycota species *Phanerodontia chrysosporium* (PC,**
226 **orange) and *Paxillus involutus* (PI, yellow). The symbols denote incubations with glucose (circles), succinate (squares), tannic acid**
227 **(diamonds), or β-cyclodextrin (triangles).**

228

229 The growth substrates induced a wide range in CUE values, ranging from 0.1 to 0.6 (Fig. 2). Higher CUE values were typically
230 observed for Ascomycota and ~~Zycomycota~~ Zygomycota species growing on glucose, and lower values for their growth on
231 succinate and tannic acid. CUE estimated for Basidomycota species was always low (< 0.15). The CUE range for growth on
232 glucose (0.1-0.6), β-cyclodextrin (0.1-0.6), and succinate (0.2-0.5) were larger than observed for tannic acid (0.15-0.3).
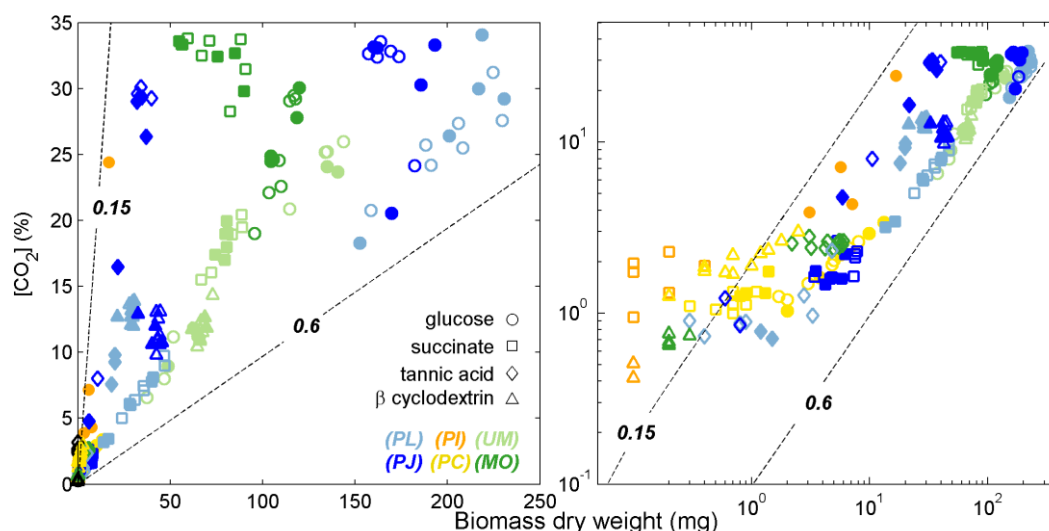

233

234 **Figure 2. Accumulation of biomass and headspace CO_2 for fungal species from three phyla growing on monomers or**
235 **complex substrates. The right panel includes the same data on a log-log scale to depict the trends of fungi exhibiting**
236 **minimal growth. Lines indicate CUE trajectories of 0.15 or 0.6, and were calculated assuming that fungal biomass**
237 **was 44% C (w/w). Colors and symbols are redundant with Fig. 1. Filled symbols indicate samples that were analyzed**
238 **by Pyr-GC-IRMS.**

239 **3.2 Stable isotopic composition of fungal lipids**

240 Fungal respiration of the different (unlabeled) growth substrates led to decreasing $\delta^{13}C$-CO_2 values as fungal biomass was
241 produced, which followed a hyperbolic trend expected for the mixing of CO_2 from two different sources (Text S1; c.f., Kendall

and Caldwell, 1998). The atom % ^{13}C in control incubations with no fungal inoculum was measured at the latest time of harvest of inoculated incubations and stayed below 0.4%, except for incubations with tannic acid, where it ranged between 2% and 3%; the $\delta^{13}C$ values of the substrates were glucose = -26.5‰; succinate = -28.3‰, tannic acid = -27.4‰, β-cyclodextrin = -10.6‰. The mixing relationship was modeled using all CO_2 data, across all incubations, and integrated to approximate the mixing-weighted average ^{13}F value of IC for each incubation (cf., Text S1, Fig. S2), which was finally applied in the denominator of Eq. 1 to estimate the fraction of lipid-C derived from IC. For incubations that produced sufficient fungal biomass for stable C isotopic analysis, the weighted average $\delta^{13}C$ values of IC that were applied in Eq. 1 ranged from 200 to 1400 ‰ (i.e., ~ 1.3 to 2.6 AT% ^{13}C), and was largely dependent on how much of the substrate was respired to CO_2.

3.2.1 Carbon isotopes

The $\delta^{13}C$ values of fungal biomarker fatty acid $C_{18:2}$ (Table 1) produced under natural cultivation conditions with glucose (i.e., non-labeled; AT%$_{DIC}$ ~ 1%) ranged from -24.1‰ to -21.2‰ across all strains (n = 6 species). As expected, $C_{18:2}$ harvested from the labeled incubations exhibited slightly higher $\delta^{13}C$ values (up to +11‰; PC grown on glucose) than the corresponding experiment amended with natural bicarbonate, likely owing to the incorporation of labeled IC into the $C_{18:2}$ fatty acid.

Table 1: $\delta^{13}C$ values of fungal biomarker $C_{18:2}$ harvested from incubations with non-labeled substrates (nat) or those amended with ^{13}C-labeled bicarbonate. Incorporation of inorganic C (%IC) was calculated based on Eq.1. Errors represent the standard deviation of replicate incubations. Not all fungal species grew sufficiently on all substrates and thus %IC could not have been determined (n.d).

Species	Glucose $\delta^{13}C$ (‰)		IC (%)	Succinate $\delta^{13}C$ (‰)		IC (%)	Tannic acid $\delta^{13}C$ (‰)		IC (%)	β-cyclodextrin $\delta^{13}C$ (‰)		IC (%)
	nat	+		nat	+		nat	+		nat	+	
Paxillus involutus (PI)	-21.5	-16.7	0.6 (±0.2)	n.d	n.d	n.d	n.d	n.d	n.d	n.d	n.d	n.d
Phanerodontia chrysosporium (PC)	-24.1	-15.9	0.9 (±0.3)	-27.3	-23.5	0.3 (±0.1)	n.d	n.d	n.d	n.d	n.d	n.d
Mortierella (MO)	-21.9	-20.7	0.5 (±0.1)	-31.7	-31.5	0.1 (±0.1)	n.d	n.d	n.d	n.d	n.d	n.d
Umbelopsis (UM)	-21.2	-21.1	0.1 (±0.0)	-30.6	-28.2	0.7 (±0.2)	n.d	n.d	n.d	-21.7	-18.1	0.8 (±0.3)
Penicillium janczewskii (PJ)	-23.2	-22.1	0.5 (±0.2)	-30.1	-27.8	0.2 (±0.0)	-25.9	-20.5	2.2 (±0.5)	-20.7	-20.1	0.1 (±0.2)
Paecilomyces lilacinus (PL)	-23.0	-23.5	n.d	-30.8	-29.9	0.1 (±0.0)	-25.4	-25.0	0.1 (±0.0)	-19.1	-17.6	0.7 (±0.4)

262 The estimated incorporation of IC into $C_{18:2}$ (%IC) typically ranged up to 1%; only PJ grown on tannic acid exhibited higher

263 %IC values, which ranged up to 2.2% (Table 1, Fig. 3). There were no general trends observed in %IC with other measured or

264 estimated parameters, including CUE; however, for the two species that were able to grow on tannic acid, %IC was positively

265 correlated with the amount of CO_2 and biomass produced during the incubation ($R^2 > 0.85$, n = 5, p < 0.01).
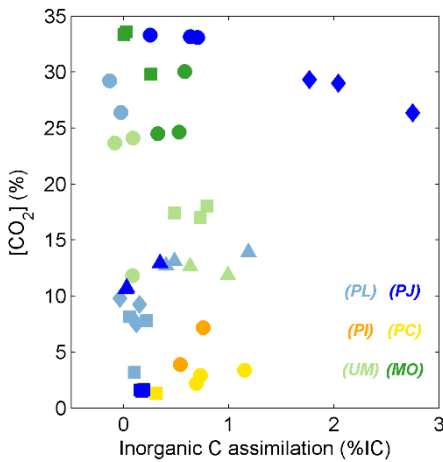

266

267

268 **Figure 3. %IC values for fungal species respiring glucose (circles), succinate (squares), tannic acid (diamonds), or β-**

269 **cyclodextrin (triangles). Colors represent individual fungal isolates as described in Fig. 1.**

270

271

272 **3.2.2 Water assimilation factor (a~~w~~a_w)**

273 The "net" contribution of water hydrogen to lipid H is reported as the water hydrogen assimilation factor a~~w~~ a_w (Kopf et al.,

274 ~~2015~~2016), and was estimated based on the slope of the linear regression line between H isotopic composition of lipid versus

275 growth medium water (Fig. 4), which ranged from natural MilliQ (δ^2H = -45‰ ± 10‰) to the labeled treatments (65‰ ± 4‰;

276 166‰ ± 10‰; 368‰ ± 27‰). The a~~w~~ a_w values for the fungal biomarker $C_{18:2}$ grown on glucose ranged from 0.37 ± 0.03 to

277 0.75 ± 0.06 with an average value of 0.60 ± 0.05 (n = 6 species; ±SEM). When grown on succinic acid, the a~~w~~ a_w values for

278 $C_{18:2}$ harvested from individual species ranged from 0.78 ± 0.01 to 0.96 ± 0.02 with an average value of 0.83 ± 0.04 (n = 4

279 species; ±SEM). When grown on tannic acid, the a~~w~~ a_w values for $C_{18:2}$ harvested from individual species ranged from 0.74 ±

280 0.06 to 0.77 ± 0.03, and when grown on β-cyclodextrin the a~~w~~ a_w values for $C_{18:2}$ ranged from 0.46 ± 0.03 to 0.68 ± 0.04 with

281 an average value of 0.58 ± 0.06 (n = 4 species; ±SEM). The average a~~w~~ a_w values for $C_{18:2}$ for all substrates and species was

282 0.67 ± 0.04 (±SEM).

283

3.2.3 H isotope fractionation factors $\alpha_{C18:2/water}$ and $\varepsilon_{C18:2/water}$

The range of traditionally reported isotope effects $\alpha_{C18:2/water}$ and $\varepsilon_{C18:2/water}$ (Sessions and Hayes, 2005) for all natural and [2]H-labeled fungal growth experiments was 0.73 to 1.08 and -265 to +83 ‰, respectively (Table S1). PL growth on tannic acid exhibited the highest values (0.97 to 1.08 and -35 to +83 ‰, respectively; Fig. 5, Table S1), while for all other growth experiments, $\alpha_{C18:2/water}$ and $\varepsilon_{C18:2/water}$ remained < 0.94 and -65 ‰, respectively. Considering only the growth experiments performed without label addition, Tthe average (±SD) $\varepsilon_{C18:2/water}$ values were not significantly different for fungi growing on glucose (-~~151~~ 115 ± ~~121~~34 ‰, n = ~~6~~13), succinate (-~~121~~ 111 ± ~~44~~35 ‰, n = ~~4~~8), ~~tannic acid (39 ± 63 ‰, n = 2),~~ or β-cyclodextrin (-~~171~~133 ± ~~82~~7‰, n = ~~3~~6), but growth on~~.~~ tannic acid elicited significantly higher values (+12 ± 81 ‰, n = 5; p < 0.01, two-tailed homoscedastic t-test), Within species comparisons revealed that both Zygomycota species (*Mortierella* and *Umbelopsis*) exhibited significantly more negative $\varepsilon_{C18:2/water}$ values when grown on succinate (-127±6 and -155±8 ‰, n = 2) versus glucose (-78±3 and -127±5 ‰, respectively, n = 2; p < 0.05). The only other significant differences in $\varepsilon_{C18:2/water}$ values were observed for growth of the Ascomycota species *P. lilanicus*, for which growth on tannic acid (+71±18 ‰, n = 3) yielded higher values than on glucose (-122±15 ‰, n = 2), succinate (-84±6 ‰, n = 2), and β-cyclodextrin (-132±2 ‰, n = 2; all p < 0.01); the $\varepsilon_{C18:2/water}$ values for growth on succinate and β-cyclodextrin were also significantly different (p < 0.01).

298

299
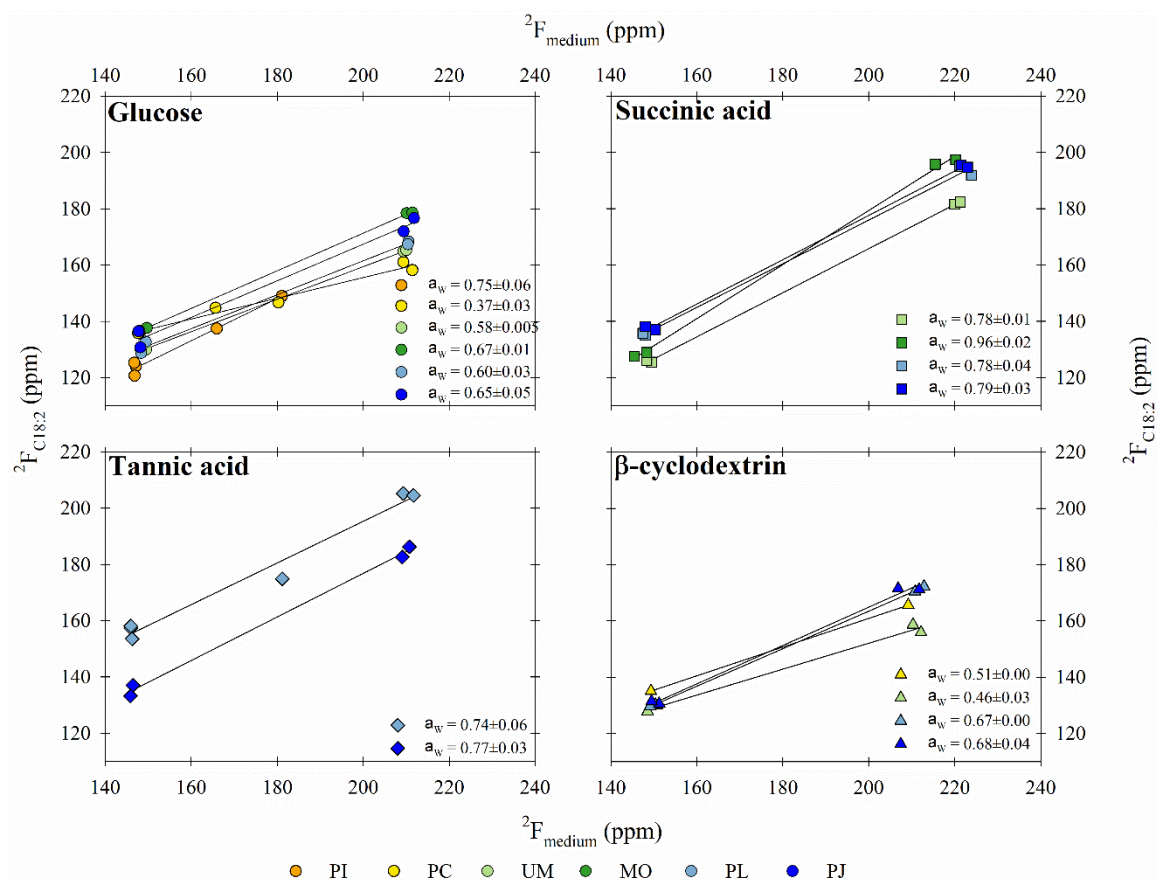
Figure 4. The water hydrogen assimilation factor (~~a~~$_w$-$\underline{a_w}$ values) estimated as the slope of the fractional $^{2/1}$H abundance (^{2}F) in lipids (y-axis) versus medium water (x-axis). Data are shown for fungal biomarker $C_{18:2}$ produced during growth on the different substrates (glucose, succinic acid, tannic acid and β-cyclodextrin) and harvested from the different fungal isolates *[Paxillus involutus* (PI), *Phanerodontia chrysosporium* (PC), *Mortierella* sp. (MO), *Umbelopsis* sp. (UM), *Penicillium janczewskii* (PJ), and *Paecilomyces lilacinus* (PL)]. R^2 values for all slopes were > 0.97.
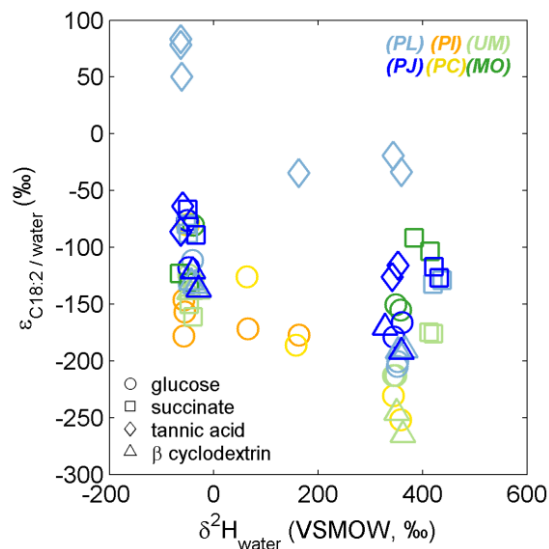
Figure 5. The apparent isotope effect ($\varepsilon_{C18:2/water}$) for fungi grown in medium having variable δ^2H_{water} composition. The colors and symbols are redundant with Fig. 1. For each species-substrate pair, the large range and/or decrease in $\varepsilon_{C18:2/water}$ in ^{2}H-enriched medium are expected, given the additional contributions of substrate-H and metabolic water-H to lipid-H during biosynthesis.

4 Discussion

4.1 Fungal growth dynamics

Collectively, the fungal incubation experiments included six species representing three different phyla growing on one of four substrates, and exhibited a large range in the relative amounts of CO_2 (0.2-34% v/v) and biomass produced (0-230 mg dry weight; Fig. 1), with CUE ranging from 0.15 to 0.6 (Fig. 2). While atmospheric, oxic conditions likely prevailed during most of the incubation period, it is probable that some incubations turned anoxic when CO_2 levels exceeded 21%, which occurred in incubations of Ascomycota and Zygomycota growing on glucose, Ascomycota growing on tannic acid, and Zygomycota growing on succinate. The accumulation of CO_2 was necessary consequence of performing the incubations in closed bottles, which was required to prevent the escape of ^{13}C-labeled IC and also to prevent microbial contaminations. Nevertheless, such alteration between oxic and anoxic conditions is common in natural environments, and the measured IC assimilation into fungal lipids was consistently low (< 3%; Fig. 3), regardless the implied anoxia. Furthermore, the observed variability in CUE, %IC, and ~~a_w~~ $\underline{a_w}$ between growth experiments were not correlated with large increases in headspace CO_2.

4.2 Fungal IC assimilation into lipids

14

330 A fundamental process in nature and basis for ecological food webs is the fixation of IC via photosynthesis and/or

331 chemosynthesis by autotrophic organisms. The IC assimilation by heterotrophic organisms also plays an important role in

332 ensuring the provision of energy and to replenish intermediates in the TCA cycle that have been released for biosynthesis

333 (Kornberg 1965). Therefore, IC assimilation is a proxy for both anabolic processes and the catabolic status of the cell,

334 influenced by assimilation, biosynthesis, anaplerotic reactions, and redox balancing reactions (Braun et al., 2021; Erb 2011).

335 Previous reports on the by-fixation of IC (%IC) via anaplerotic pathways into heterotrophic biomass varied between 1% and

336 8% (Dijkhuizen & Harder, 1985; Feisthauer et al., 2008; Romanenko 1964; Roslev et al., 2004), whereas for fungi it was

337 previously reported to amount to roughly 1% (Sorokin 1961; Schinner & Concin, 1981; Schinner et al., 1982), and was recently

338 shown to vary between 2% and 12% for Ascomycota when grown on glucose or glutamic acid (Jabinski et al., 2024). Our

339 results, focusing on a specific fatty acid biomarker, demonstrate a low range in %IC for all different substrates and species

340 tested in this study (0 - 3%), with the Ascomycota (0 - 2%) assimilating relatively less IC than previously reported species

341 (4.6% ± 1.6%; Jabinski et al., 2024). The highest observed incorporation was 2.2 ± 0.5% by *Penicillium janczewskii* (PJ, n =

342 3) when grown for 21 days on tannic acid (Table 1; Fig. 3). Only the other Ascomycota species, *Paecilomyces lilacinus* (PL),

343 grew sufficiently on tannic acid (up to 10% CO_2 and 20 mg dry weight after 13 days; %IC = 0.14 ± 0.02%, n = 3 ; Figs. 1, 3),

344 suggesting that increased assimilation of IC by PJ may have occurred during the extra week of incubation and promoted higher

345 biomass production. The high CO_2 levels also suggest that the incubations of PJ with tannic acid may have turned anoxic,

346 which may also explain the higher IC incorporation in these incubations. Overall, heterotrophic IC assimilation does not appear

347 to be a hallmark of any of the variety of fungal taxa or catabolic pathways probed in this study.

348

349 **4.3 Water hydrogen incorporation into fungal lipid biomarker $C_{18:2}$**

350 As demonstrated previously, the regression slope between hydrogen isotopic composition of water medium and microbial lipids

351 (i.e., a_w) varies with the type of metabolism (Zhang et al., 2009; Valentine, 2009; Wijker et al., 2019; Jabinski et al., 2024),

352 and importantly for heterotrophs, a non-negligible proportion of hydrogen may derive from sources other than ambient water.

353 For fatty acid biosynthesis, H incorporation is suggested to be a function of transporters and electron acceptors (NADPH and

354 NADH), with contributions accounting for around half of all lipid hydrogen (Maloney et al., 2024). The remaining comprises

355 equal contributions of H obtained directly from environmental water or acetyl-CoA (Valentine, 2009; Zhang et al., 2009; Caro

356 et al., 2023). The consensus from previous studies that investigated the lipids of heterotrophic bacteria is that microbial

357 heterotrophs exhibit a_w values ranging from 0 to 1, with a mean of 0.71±0.17 (e.g., Caro et al., 2023), though some organisms

358 have exhibited a_w values exceeding 1 (Dirghangi et al., 2013; Jabinski et al., 2024). Jabinski et al. (2024) demonstrated that

359 five species of heterotrophic Ascomycota exhibit similar a_w values (0.62 ± 0.04) for the fungal biomarker $C_{18:2}$ during growth

360 on glucose. Zhang et al. (2009) reported similar a_w values for *E.coli* grown on glucose (0.63 ± 0.03). In the current study,

361 a_w values for the fungal biomarker $C_{18:2}$ during growth on glucose (0.60 ± 0.05) were agreeable with Jabinski et al. (2024),

362 but more variable, likely owing to the broader phylogenetic coverage of the current study.

The ~~similarly~~ large variability in $\varepsilon_{C18:2/water}$ ~~values~~estimates (Fig. 5; Table S1) can be partly attributed to the large range in δ^2H of medium water, which contributes H together with the substrate and metabolic water to determine $\delta^2H_{C18:2}$, even though the net isotope effect ($\alpha_{C18:2/water}$) may be consistent for a specific species-substrate pair (~~Fig. 5;~~ Session and Hayes, 2005; Kopf et al., ~~2015~~2016). In other words, $\varepsilon_{C18:2/water}$ values do not account for the admixture of H sources that also affect $\delta^2H_{C18:2}$ of heterotrophic fungi ~~exhibits more inertia than δ^2H_{H2O} in highly labeled incubations, yielding lower $\varepsilon_{C18:2/water}$ values compared to natural abundance incubations~~. More robust differences were observed in ~~a_w~~a_w values both between and within the different phyla and substrates tested.

4.3.1 Trends across fungal phyla

For incubations in which the ~~investigated~~ Zygomycota isolates produced enough biomass to determine a_w (i.e., glucose, succinate, β-cyclodextrin; $n = 5$; Fig. 4), we observed a highly significant inverse correlation with CUE ($R^2 = 0.87$, p < 0.01; Fig. 6), suggesting ~~the~~coupling of ~~potential for~~ a_w ~~to serve as a proxy for~~with growth efficiency. Presumably, the proportion of substrate-derived H incorporated into lipids increases with more efficient incorporation of substrate C into biomass. Ascomycota exhibited the most consistent ~~a_w~~a_w values among phyla when grown on each of the four different substrates [0.63 ± 0.03 (glucose); 0.78 ± 0.01 (succinate); 0.76 ± 0.02 (tannic acid); 0.67 ± 0.01 (β-cyclodextrin)], but also the largest variability in CUE (0.08-0.59; Fig. 2). CUE and ~~a_w~~a_w exhibited a similar trend as observed for Zygomycota isolates, but were not significantly correlated across incubations of Ascomycota, ~~suggesting that drastic changes in the central metabolic pathways that convert C substrates to either biomass or energy reserves did not systematically alter the net water-H incorporation into lipids. This in in contrast to the prevailing notion that a_w values respond to changes in NADPH production and turnover within the cell (e.g. Wijker et al., 2019).~~ Basidiomycota only produced sufficient biomass when fed ~~mycota~~substrates that activated the glycolytic pathway (glucose or β-cyclodextrin; CUE < 0.3), yet showed high variability in ~~a_w~~a_w between species (0.37 ± 0.03 < ~~a_w~~a_w < 0.75 ± 0.06; Fig. 4), which were beyond the more confined range of ~~a_w~~a_w values determined for isolates belonging to Zygomycota and Ascomycota. ~~For incubations in which the investigated Zygomycota isolates produced enough biomass to determine a_w (i.e., glucose, succinate, β-cyclodextrin; $n = 5$; Fig. 4), we observed a highly significant inverse correlation with CUE ($R^2 = 0.87$, p < 0.01; Fig. 6), suggesting the potential for a_w to serve as a proxy for growth efficiency.~~
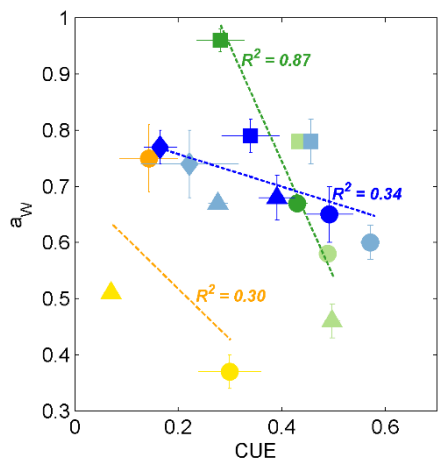
Figure 6. Biplot of CUE and ~~aw~~ $\underline{a_w}$ values for fungi growing on glucose (circles), succinate (squares), tannic acid (diamonds), or β-cyclodextrin (triangles). The colors are redundant with Fig. 1, representing the phlya Ascomycota (blue shades, $n = 8$), Zygomycota (green shades, $n = 5$), and Basidiomycota (yellow and orange symbols, $n = 3$). The dashed lines and R^2 values indicate the linear regression for the corresponding phylum across all substrates that yielded sufficient biomass. Only the regression for Zygomycota was significant ($p < 0.01$).

4.3.1 Trends across C substrates

Across all incubations, the similar ~~aw~~ $\underline{a_w}$ values determined for growth on glucose (0.60 ± 0.05) versus β-cyclodextrin (0.58 ± 0.06), of which the latter consists of seven glucopyranose units ($C_6H_{12}O_6$), suggests that the catabolism of glucose subunits via glycolysis overprints signals of water-H incorporation that may derive during degradation of the β-cyclodextrin oligomer. Alternatively to glycolysis, succinate yielded significantly higher ~~aw~~ $\underline{a_w}$ values (0.83 ± 0.05), which was in the same range as reported for *~~C. oxalaticus~~ $\underline{E. coli}$* when grown on succinate (~~aw~~ $\underline{a_w}$ 0.80 ± 0.05; Zhang et al., 2009), and was more similar to that reported previously for fungal growth on glutamic acid (0.90 ± 0.07; Jabinski et al., 2024). Considering all fungal incubations, a one-way analysis of variance (ANOVA; Holm-Sidak method; SigmaPlot v11) confirmed the significant difference in ~~aw~~ $\underline{a_w}$ values between growth on glucose and glutamic acid ($p < 0.001$), glutamic acid and β-cyclodextrin ($p < 0.001$), succinate and glucose ($p < 0.003$), and succinate and β-cyclodextrin ($p < 0.005$). It also confirmed that there was no significant difference between the other substrate combinations ($p > 0.05$).

Glutamic acid and succinate are thought to be introduced into the TCA cycle through coupled metabolites, where succinate is a direct metabolite of the TCA cycle and glutamic acid is converted to α-ketoglutarate by transamination before entering the TCA cycle, which is only 2 steps from succinate (Cooper et al., 2014). Also, being acids, these substrates may have a greater capacity than saccharides to exchange H with ambient water at experimental pH (typically $2 < pH < 5.2$), especially glutamic acid, which also comprises an amino moiety. Tannic acid (0.76 ± 0.02) yielded no significant differences ($p > 0.05$) from the other substrates, and is reported to be degraded to different subunits including gallic acid and glucose (Banerjee and Mahapatra,

17

413 2012; Lekha and Lonsane, 1997 and references within). Aromatic degradation pathways employed by fungi generate

414 intermediates that go through the β-ketoadipate pathway (Mäkelä et al., 2015) before entering the TCA cycle as a succinyl-

415 CoA metabolite (Lekha and Lonsane, 1997). The ~~a_w~~ a_w values induced by degradation of tannic acid suggest that it integrates

416 both the lower ~~a_w~~ a_w signature of glycolysis and higher ~~a_w~~ a_w signature of the TCA cycle (Fig. 7). ~~Similarly to trends in a_w,~~

417 ~~the $\varepsilon_{C18:2/water}$ values estimated for fungal growth on succinate or tannic acid were typically higher than glucose or β-~~

418 ~~cyclodextrin, for a given δ^2H_{H2O} treatment (Fig. 5; Table S1).~~

419 Together, our incubation experiments suggest that ~~a_w~~ a_w values determined for the fungal biomarker $C_{18:2}$ could not distinguish

420 between fungal growth on relatively labile monomers (i.e., glucose and succinate; requiring as few as 5 days of cultivation)

421 versus larger, less-labile substrates (i.e., β-cyclodextrin and tannic acid; requiring 20 to 183 days of cultivation). However, ~~a_w~~

422 a_w values of fungal lipid biomarkers may be indicative of fungi employing primarily glycolytic or TCA pathways.

423 Environmental assays that quantify fungal lipid production via the incorporation of ambient water-H (i.e., the lipid-SIP

424 approach) may upscale to total production estimates by applying our calculated mean ~~a_w~~ a_w value of 0.69 ± 0.03 [n = 27; ±

425 (SEM)], which is consistent with the ~~a_w~~ a_w value of 0.71 recommended for soil microbial communities (Caro et al., 2023). For

426 ^{2}H-SIP investigation of fungal ecotypes supplied with TCA metabolites, such as mycorrhiza, the ~~a_w~~ a_w value of $C_{18:2}$ may range

427 up to 0.83 ± 0.05. Similar approaches could be applied to environmental samples, such that the ~~a_w~~ a_w values of phospholipids

428 containing C18:2 fatty acids could inform the distribution of predominant metabolic ecotypes across a soil profile.

429 Comparisons of net $^{2/1}$H fractionation factors (i.e., $\varepsilon_{18:2/H2O}$; Table S1) estimated in the current study to previous reports are

430 most relevant for those derived from our natural abundance incubations. However, we note that these estimates were

431 determined for a fewer number of replicates (n = 2 or 3) and represent the distinct value relative to our laboratory water (δ^2H

432 = -49 ‰), which varies from labeled treatments (Table S1) and likely natural systems having a significantly different δ^2H_{H2O}.

433 Fungal isolates that could successfully grow on tannic acid exhibited the highest $^2\varepsilon_{18:2/H2O}$ values, which is likely manifested

434 by NADPH production and turnover (e.g. Wijker et al., 2019). The Zygomycota isolates investigated in the current study

435 (*Mortierella* and *Umbelopsis*) both exhibited relatively strong fractionation of $^{2/1}H_{water}$ during growth on succinate ($\varepsilon_{18:2/H2O} \leq$

436 -123 ‰), which contrasts the trends observed for Ascomycota isolates and previous reports of heterotrophic bacteria (e.g.,

437 Zhang et al., 2009), where $\varepsilon_{18:2/H2O}$ values are typically higher for succinate relative to other C substrates. Together, the relatively

438 strong $^{2/1}$H fractionation (i.e., low $\varepsilon_{18:2/H2O}$) and high water isotope incorporation efficiency (a_w) suggest these Zygomycota

439 isolates employ an alternative catabolic pathway for succinate, resulting in minor incorporation of succinate-derived H into

440 $C_{18:2}$.

4.4 Dual-SIP approach

444 Dual-SIP experiments with ^2H_2O and ^{13}C-dissolved IC previously highlighted the potential to track microbial activity and

445 distinguish heterotopic vs autotrophic metabolic modes within environmental settings and pure cultures (Kellerman et al.,

2012, 2016; Wegener et al., 2012; Huguet et al., 2017; Wu et al., 2018, 2020). This approach was also previously applied to investigate fungal pure cultures (Jabinski et al., 2024), in which the plot of assimilation of IC versus water-H into the fungal biomarker $C_{18:2}$ could distinguish five Ascomycota species growing on glucose or glutamic acid, with a_w-a_w values explaining most of the variability. While calculated IC:a_w a_w are useful to distinguish autotrophic from heterotrophic growth (cf. Wegener et al., 2016), all calculated values in this study remained near zero, with %IC ranging up to 3% and a_w-a_w values ranging from 0.37 to 0.96 (Fig. 4). This pure culture study therefore suggests that fungal assimilation of IC is low and less insightful than the more distinguishable a_w–a_w values for identifying the relative contributions of fungal phylotypes or ecotypes in environmental assays.
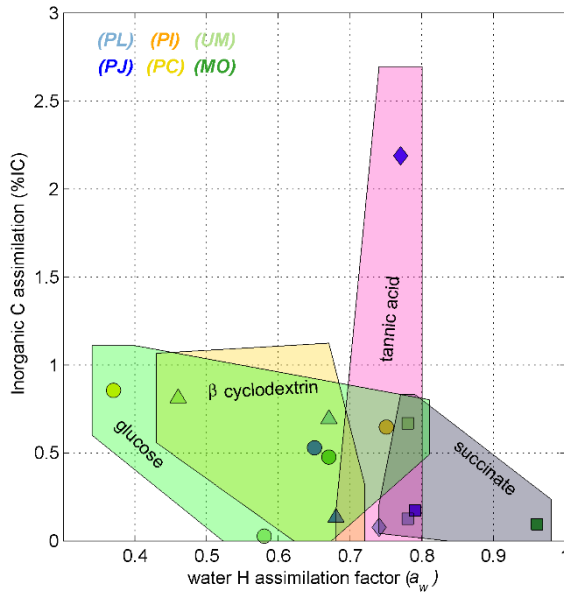
Figure 7. Scatterplot of %IC and a_w-a_w **values plot for** $C_{18:2}$ **harvested from incubations of Ascomycota (blue symbols), Basidiomycota (yellow and orange symbols), and Zygomycota (green symbols). The shaded polygons span the range of %IC and** a_w-a_w **values (±** **propagated error) for fungal growth on glucose (circles, green shape), succinate (squares, grey shape), tannic acid (diamonds, pink** **shape), or β-cyclodextrin (triangles, yellow shape). Each data point represents one species-substrate pair determined for** *n* > 4 **growth** **experiments.**

5 Conclusion

The purpose of this work was to apply the dual-SIP assay on pure fungal cultures to define the effect of different organic C substrates on the incorporation of water-H and IC into their membrane lipids. Although heterotrophic CO_2 fixation by microbes

464 may range up to 8% of biomass C, the IC assimilation into the fungal biomarker $C_{18:2}$ harvested from six species representing

465 Ascomycota, Basidiomycota, and Zygomycota did not vary consistently between species or substrate, and remained below

466 3%. Our findings suggest that the fungal catabolic pathways activated by the variety of substrates tested in this study cannot

467 fully account for the higher levels of heterotrophic CO_2 incorporation reported in natural systems. However, *Penicillium*

468 *janczewskii*, the species that was most successful at respiring tannic acid, also exhibited the highest %IC value of all incubations

469 (Fig. 3; Fig. 7), suggesting that fungal degradation of similarly complex substrates may rely in part on the assimilation of IC

470 (e.g., via anaplerotic reactions). The use of SIP to estimate %IC of heterotrophs required (*i*) a closed system to prevent loss of

471 ^{13}C label to the atmosphere, and (*ii*) a high label dose, to contend with the accumulation of CO_2 respired from growth substrate.

472 These conditions intensified upon decreases in pH during the growth experiments, thereby shifting the speciation of IC toward

473 CO_2, which may have further, yet unknown consequences for anaplerotic incorporation of the IC. Future applications to

474 determine %IC for microbial heterotrophs should consider repeated spiking or continuous cultivation practices to better

475 stabilize pH and $\delta^{13}C_{DIC}$. Likewise, it would be worth considering isotopic analyses of other potential bioindicator compounds

476 (e.g., sterols, peptides, aminosugars) to see whether incorporation of the IC into such other compounds would render higher

477 levels than fatty acids.

478 In contrast to %IC, we conclude that substrates that activated the glycolysis pathway yielded significantly lower ~~a_w~~ a_w values

479 than those catabolized as TCA intermediates. The relatively high $\varepsilon_{18:2/H2O}$ values harvested from fungi grown on tannic acid

480 may further help to distinguish fungal ecotypes growing on complex, aromatic-containing substrates in natural systems. The

481 expanded a_w dataset reported in this study suggests that the accuracy of fungal production estimated by ^2H-lipid SIP

482 experiments can be improved by applying the average ~~a_w~~ a_w value of 0.69 for saprotrophic fungi or up to 0.83 for

483 mycorrhizal fungi. Furthermore, determination of ~~a_w~~ a_w values in environmental ^2H-SIP assays may be useful to identify the

484 relative contributions of fungal ecotypes that rely on C substrates fueling glycolysis (e.g., leaf litter) versus those that are fed

485 primarily by TCA intermediates (e.g., root or microbial exudates). Lastly, to our knowledge, the two Zygomycota strains

486 investigated in this study provide the first evidence of a potential correlation between ~~a_w~~ a_w and CUE (Fig. 6), encouraging

487 further exploration of the link between these two parameters, both of which are coupled to microbial central metabolic

488 pathways.

489

490 **Data availability**

491 Data presented in the figures and tables are available in supplementary material (Table S1) and will be made available on the

492 Fractome Database (https://fractome.caltech.edu/).

493

494 **Author contribution**

495 Stanislav Jabinski, Conceptualization, Data curation, Formal analysis, Investigation, Methodology, Software, Validation,

496 Visualization, Writing – original draft, Writing – review and editing

497 Vítězslav Kučera, Investigation, Methodology, Resources, Writing – review and editing

498 Marek Kopáček, Formal analysis, Methodology, Resources, Validation,

499 Jan Jansa, Conceptualization, Formal analysis, Methodology, Resources, Validation, Writing – review and editing

500 Travis B. Meador, Conceptualization, Data curation, Formal analysis, Funding acquisition, Investigation, Methodology, Project
501 administration, Resources, Software, Supervision, Validation, Visualization, Writing – original draft, Writing – review and
502 editing

Competing interests

504 The authors declare that they have no conflict of interest.

Disclaimer Acknowledgements

515

516

517

518

519

References

Baldrian, P., Voříšková, J., Dobiášová, P., Merhautová, V., Lisá, L., & Valášková, V. Production of extracellular enzymes and degradation of biopolymers by saprotrophic microfungi from the upper layers of forest soil. *Plant and Soil,* 338(1-2), 111-125. doi:10.1007/s11104-010-0324-3, 2011.

Banerjee, D., & Mahapatra, S. Fungal tannase: a journey from strain isolation to enzyme applications. *Dyn Biochem Process Biotechnol Mol Biol,* 6(2), 49-60, 2012.

Boer, W. D., Folman, L. B., Summerbell, R. C., & Boddy, L. Living in a fungal world: impact of fungi on soil bacterial niche development. *FEMS microbiology reviews,* 29(4), 795-811, 2005.

Boschker HTS, Middelburg JJ. Stable isotopes and biomarkers in microbial ecology. *FEMS Microbiol Ecol* 40:85–95. https://doi.org/10. 1111/j.1574-6941.2002.tb00940.x 2002.

Boschker, H. T. S., Nold, S. C., Wellsbury, P., Bos, D., De Graaf, W., Pel, R., ... & Cappenberg, T. E. . Direct linking of microbial populations to specific biogeochemical processes by 13C-labelling of biomarkers. *Nature,* 392(6678), 801-805, 1998.

Braun A, Spona-Friedl M, Avramov M, Elsner M, Baltar F, Reinthaler T, Herndl GJ, Griebler C. Reviews and syntheses: heterotrophic fixation of inorganic carbon–significant but invisible flux in environmental carbon cycling. *Biogeosciences* 18:3689–3700. https://doi.org/10. 5194/bg-18-3689-2021, 2021.

Bukovská P, Bonkowski M, Konvalinková T, Beskid O, Hujslová M, Püschel D Utilization of organic nitrogen by arbuscular mycorrhizal fungi-is there a specific role for protists and ammonia oxidizers? Mycorrhiza. ;28(3):269–83. https://doi.org/10.1007/s00572-018-0825-0, 2018.

Canarini, A., Fuchslueger, L., Schnecker, J., Metze, D., Nelson, D. B., Kahmen, A., ... & Richter, A. Soil fungi remain active and invest in storage compounds during drought independent of future climate conditions. *Nature Communications*, *15*(1), 10410, 2024.

Carlson C.A., N.R. Bates, D.A. Hansell, D.K. Steinberg. Carbon Cycle. In: J. Steele, S. Thorpe, K. Turekian (Eds.) Encyclopedia of Ocean Science, 2nd Edition. Academic Press, 477-486, 2001.

Caro, T. A., McFarlin, J., Jech, S., Fierer, N., & Kopf, S. Hydrogen stable isotope probing of lipids demonstrates slow rates of microbial growth in soil. Proceedings of the National Academy of Sciences, 120(16), e2211625120, 2023.

Ciais, P., Dolman, A. J., Bombelli, A., Duren, R., Peregon, A., Rayner, P. J., . . . Marland, G. Current systematic carbon-cycle observations and the need for implementing a policy-relevant carbon observing system. Biogeosciences, 11(13), 3547-3602. doi:10.5194/bg-11-3547-2014, 2014.

Cooper AJL, Kuhara T. α-Ketoglutaramate: an overlooked metabolite of glutamine and a biomarker for hepatic encephalopathy and inborn errors of the urea cycle. Metab Brain Dis 29:991–1006. https:/ /doi.org/10.1007/s11011-013-9444-9, 2014.

Dijkhuizen, L., & Harder, W. Microbial metabolism of carbon dioxide. Comprehensive biotechnology: the principles, applications, and regulations of biotechnology in industry, agriculture, and medicine/editor-in-chief, Murray Moo-Young, 1985.

554 Dumont, M. G., & Murrell, J. C. Stable isotope probing—linking microbial identity to function. Nature Reviews Microbiology,
555 3(6), 499-504, 2005.

556 Erb TJ. Carboxylases in natural and synthetic microbial pathways. Appl Environ Microbiol 77:8466–8477.
557 https://doi.org/10.1128/AEM. 05702-11, 2011.

558 Feisthauer, S., Wick, L. Y., Kästner, M., Kaschabek, S. R., Schlömann, M., & Richnow, H. H. Differences of heterotrophic
559 13CO2 assimilation by Pseudomonas knackmussii strain B13 and Rhodococcus opacus 1CP and potential impact on biomarker
560 stable isotope probing. Environmental Microbiology, 10(6), 1641-1651, 2008.

561 Fioretto, A., Di Nardo, C., Papa, S., & Fuggi, A. Lignin and cellulose degradation and nitrogen dynamics during decomposition
562 of three leaf litter species in a Mediterranean ecosystem. Soil Biology and Biochemistry, 37(6), 1083-1091.
563 doi:10.1016/j.soilbio.2004.11.007, 2005.

564 Fischer, C. R., Bowen, B. P., Pan, C., Northen, T. R., & Banfield, J. F. Stable-isotope probing reveals that hydrogen isotope
565 fractionation in proteins and lipids in a microbial community are different and species-specific. ACS chemical biology, 8(8),
566 1755-1763, 2013.

567 Frey, S. D. Mycorrhizal fungi as mediators of soil organic matter dynamics. Annual review of ecology, evolution, and
568 systematics, 50, 237-259. doi:10.1146/annurev-ecolsys-110617-062331, 2019.

569 Grinhut, T., Hadar, Y., & Chen, Y. Degradation and transformation of humic substances by saprotrophic fungi: processes and
570 mechanisms. Fungal biology reviews, 21(4), 179-189, 2007.

571 Hayes, J. M. An introduction to isotopic calculations. Woods Hole Oceanographic Institution, Woods Hole, MA, 2543, 2004.

572 Hoefs, J. Stable isotope geochemistry. Springer International Publishing AG, part of Springer Nature. doi:10.1007/9783-319-
573 78527-1, 2018.

574 HoÈgberg, P., Nordgren, A., Buchmann, N., Taylor, A. F., Ekblad, A., HoÈgberg, M. N., . . . Read, D. J. Large-scale forest
575 girdling shows that current photosynthesis drives soil respiration. Nature, 411(6839), 789-792, 2001.

576 Huguet, A., Meador, T. B., Laggoun-Défarge, F., Könneke, M., Wu, W., Derenne, S., & Hinrichs, K.-U. Production rates of
577 bacterial tetraether lipids and fatty acids in peatland under varying oxygen concentrations. Geochimica et
578 Cosmochimica Acta, 203, 103-116. doi:10.1016/j.gca.2017.01.012, 2017.

579 Jabinski, S., d. M. Rangel, W., Kopáček, M., Jílková, V., Jansa, J., & Meador, T. B. Constraining activity and growth substrate
580 of fungal decomposers via assimilation patterns of inorganic carbon and water into lipid biomarkers. Applied and
581 Environmental Microbiology, 90(4), e02065-23, 2024.

582 Kellermann, M. Y., Wegener, G., Elvert, M., Yoshinaga, M. Y., Lin, Y.-S., Holler, T., . . . Hinrichs, K.-U. Autotrophy as a
583 predominant mode of carbon fixation in anaerobic methane-oxidizing microbial communities. Proceedings of the National
584 Academy of Sciences, 109(47), 19321-19326. doi:10.1073/pnas.1208795109, 2012.

585 Kellermann, M. Y., Yoshinaga, M. Y., Wegener, G., Krukenberg, V., & Hinrichs, K.-U. Tracing the production and fate of
586 individual archaeal intact polar lipids using stable isotope probing. Organic Geochemistry, 95, 13-20.
587 doi:10.1016/j.orggeochem.2016.02.004, 2016.

588 Kirk, T. K., & Farrell, R. L. Enzymatic" combustion": the microbial degradation of lignin. Annual Reviews in

589 Microbiology, 41(1), 465-501. doi:10.1146/annurev.mi.41.100187.002341, 1987.

590 Kopf, S. H., Sessions, A. L., Cowley, E. S., Reyes, C., Van Sambeek, L., Hu, Y., ... & Newman, D. K. Trace incorporation of

591 heavy water reveals slow and heterogeneous pathogen growth rates in cystic fibrosis sputum. *Proceedings of the National*

592 *Academy of Sciences*, *113*(2), E110-E116, doi: 10.1073/pnas.1512057112, 2016. ~~Kopf, S. H., McGlynn, S. E., Green-Saxena,~~

593 ~~A., Guan, Y., Newman, D. K., & Orphan, V. J. Heavy water and (15) N labelling with NanoSIMS analysis reveals growth rate~~

594 ~~dependent metabolic heterogeneity in chemostats. Environ Microbiol, 17(7), 2542-2556. doi:10.1111/1462-2920.12752, 2015.~~

595 Kornberg HL. Anaplerotic sequences in microbial metabolism. Angew Chem Int Ed Engl 4:558–565.

596 https://doi.org/10.1002/anie. 196505581, 1965.

597 Kreuzer-Martin, H. W. Stable isotope probing: linking functional activity to specific members of microbial communities. Soil

598 Science Society of America Journal, 71(2), 611-619, 2007..

599 Lekha, P. K., & Lonsane, B. K. Production and application of tannin acyl hydrolase: state of the art. Advances in applied

600 microbiology, 44, 215-260, 1997.

601 Lindahl, B. D., & Tunlid, A. Ectomycorrhizal fungi–potential organic matter decomposers, yet not saprotrophs. New

602 Phytologist, 205(4), 1443-1447. doi:10.1111/nph.13201, 2015.

603 Maloney, A. E., Kopf, S. H., Zhang, Z., McFarlin, J., Nelson, D. B., Masterson, A. L., & Zhang, X. Large enrichments in fatty

604 acid 2H/1H ratios distinguish respiration from aerobic fermentation in yeast Saccharomyces cerevisiae. *Proceedings of the*

605 *National Academy of Sciences*, *121*(20), e2310771121, 2024.

606 Osburn, M. R., Sessions, A. L., Pepe-Ranney, C., & Spear, J. R. Hydrogen-isotopic variability in fatty acids from Yellowstone

607 National Park hot spring microbial communities. Geochimica et Cosmochimica Acta, 75(17), 4830-4845, 2011.

608 Pilecky, M., Meador, T. B., Wassenaar, L.I. Advancements in Compound-Specific Hydrogen Stable-Isotope Analysis of Fatty

609 and Amino Acids. TrAC Trends in Analytical Chemistry, 118194. doi: 10.1016/j.trac.2025.118194, 2025.

610 Romanenko VI. Heterotrophic assimilation of CO2 by bacterial flora of water. Mikrobiologiia 33:679–683, 1964.

611 Roslev P, Larsen MB, Jørgensen D, Hesselsoe M. Use of heterotrophic CO2 assimilation as a measure of metabolic activity in

612 planktonic and sessile bacteria. J Microbiol Methods 59:381–393. https://doi.org/10. 1016/j.mimet.2004.08.002, 2004.

613 Sachse, D., Billault, I., Bowen, G. J., Chikaraishi, Y., Dawson, T. E., Feakins, S. J., ... & Kahmen, A. Molecular paleohydrology:

614 interpreting the hydrogen-isotopic composition of lipid biomarkers from photosynthesizing organisms. Annual Review of Earth

615 and Planetary Sciences, 40, 221-249, 2012.

616 Schinner F, Concin R, Binder H. Heterotrophic CO2 fixation by fungi in dependence on the concentration of the carbon source.

617 Paper presented at the Phyton; annales rei botanicae, 1982.

618 Schinner F, Concin R. Carbon dioxide fixation by wood-rotting fungi. Eur J For Pathol 11:120–123.

619 https://doi.org/10.1111/j.1439-0329. 1981.tb00077.x, 1981.

620 Sessions, A.L., Hayes, J.M., 2005. Calculation of hydrogen isotopic fractionations in biogeochemical systems. Geochim.

621 Cosmochim. Acta 69, 593–597.

Smith, S. E., & Read, D. Mineral nutrition, toxic element accumulation and water relations of arbuscular mycorrhizal plants. Mycorrhizal symbiosis, 3, 145-148. doi:10.1016/B978-012370526-6.50007-6, 2008.

Šnajdr, J., Cajthaml, T., Valášková, V., Merhautová, V., Petránková, M., Spetz, P., . . . Baldrian, P. Transformation of Quercus petraea litter: successive changes in litter chemistry are reflected in differential enzyme activity and changes in the microbial community composition. FEMS Microbiology Ecology, 75(2), 291-303. doi:10.1111/j.1574-6941.2010.00999.x, 2011.

Sorokin, J. I. On the carbon dioxide uptake during the cell synthesis by microorganisms. Zeitschrift für allgemeine Mikrobiologie, 6(1), 69-73. doi:10.1002/jobm.3630060107, 1966.

Sorokin, Y. I. Heterotrophic carbon dioxide assimilation by microorganisms. Zhurnal Obshchei Biologii, 22(4), 265272, 1961.

Treonis, A. M., Ostle, N. J., Stott, A. W., Primrose, R., Grayston, S. J., & Ineson, P. Identification of groups of metabolically-active rhizosphere microorganisms by stable isotope probing of PLFAs. Soil Biology and Biochemistry, 36(3), 533-537, 2004.

Valentine, D. L. Isotopic remembrance of metabolism past. Proceedings of the National Academy of Sciences, 106(31), 12565-12566. doi:10.1073/pnas.0906428106, 2009.

Warren, C. R. D2O labelling reveals synthesis of small, water-soluble metabolites in soil. *Soil Biology and Biochemistry*, *165*, 108543, 2022.

Wegener, G., Bausch, M., Holler, T., Thang, N. M., Prieto Mollar, X., Kellermann, M. Y., . . . Boetius, A. Assessing sub-seafloor microbial activity by combined stable isotope probing with deuterated water and 13C-bicarbonate. Environmental Microbiology, 14(6), 1517-1527. doi:10.1111/j.1462-2920.2012.02739.x, 2012.

Wegener, G., Kellermann, M. Y., & Elvert, M. Tracking activity and function of microorganisms by stable isotope probing of membrane lipids. Current Opinion in Biotechnology, 41, 43-52. doi:10.1016/j.copbio.2016.04.022, 2016.

Wijker, R. S., Sessions, A. L., Fuhrer, T., & Phan, M. 2H/1H variation in microbial lipids is controlled by NADPH metabolism. Proceedings of the National Academy of Sciences, 116(25), 12173-12182. doi:10.1073/pnas.1818372116, 2019.

Willers, C., Jansen van Rensburg, P. J., & Claassens, S. Phospholipid fatty acid profiling of microbial communities–a review of interpretations and recent applications. Journal of applied microbiology, 119(5), 1207-1218, 2015.

Wu W, Meador T, Hinrichs K-U. Production and turnover of microbial organic matter in surface intertidal sediments. Org Geochem 121:104–113. https://doi.org/10.1016/j.orggeochem.2018.04.006, 2018.

Wu, W., Meador, T. B., Könneke, M., Elvert, M., Wegener, G., & Hinrichs, K. U. Substrate-dependent incorporation of carbon and hydrogen for lipid biosynthesis by Methanosarcina barkeri. Environmental Microbiology Reports, 12(5), 555567. doi:10.1111/1758-2229.12876, 2020.

Zhang, X., Gillespie, A. L., & Sessions, A. L. Large D/H variations in bacterial lipids reflect central metabolic pathways. Proceedings of the National Academy of Sciences, 106(31), 12580-12586. doi:10.1073/pnas.0903030106, 2009.